EXPERIMENTAL CONFIRMATION OF CALCULATED PHASES AND ELECTRON DENSITY PROFILE FOR WET NATIVE COLLAGEN

ROBERT H. STINSON, MICHAEL W. BARTLETT, AND TEORIN KURG, *Department of Physics*
PHILLIP R. SWEENY, *Department of Microbiology, University of Guelph, Guelph, Ontario, Canada N1G 2W1*
ROBERT W. HENDRICKS, *Metals and Ceramics Division, Oak Ridge National Laboratory, Oak Ridge, Tennessee 37830 U.S.A.*

ABSTRACT An experimental procedure is developed to phase the reflections obtained in x-ray diffraction investigations of collagen in native wet tendons. Phosphotungstic acid was used for isomorphous addition in phase determination and was located by electron microscopy. Structure factors (with phases) were obtained from the electron microscopy data for the heavy metal. Structure-factor magnitudes for collagen with and without the heavy metal were obtained from the x-ray diffraction data. The first 10 orders were investigated. Standard Argand diagrams provided two solutions for each of these, except the weak sixth order. In each case, one of the two possible solutions agrees well with the phases proposed on theoretical grounds by Hulmes et al. The present results suggest that their other proposed phases are probably correct. An electron density profile along the unit cell of the fibril is presented that shows a distinct step, as expected on the basis of the hole-overlap model. The overlap region is 48% of the length of the unit cell.

INTRODUCTION

The basic structure of the tropocollagen molecule has been known for some time (1, 2). In tendon, it is normally composed of two α_1-chains and one α_2-chain. Within recent years, the primary sequence of the α_1-chain has been completely determined by the combined efforts of a number of laboratories. The sequence has been summarized by, for example, Hulmes et al. (3). The α_2-sequence has only been partially determined (4). The exact method of assembly of native tendon fibrils from these tropocollagen molecules has not been fully resolved, although the quarter-stagger, Hodge-Petruska (5) model has received considerable support (6). This model has important implications for the formation of a microfibril (7, 8). However, a minor variation of this structure has also been proposed (9), as well as a more randomized staggering (10). Also, a quarter-stagger model involving an end-to-end overlap, rather than an end-to-end gap, has been described (11, 12). Common to all of these models is an overlap and hole region in each unit cell of total length d ($d = 670$ Å) along the fibril, that would be expected to lead to a step-function in the electron density profile along the unit cell. This type of structure is apparently revealed in negative staining of fibrils where the overlap region,

Dr. Bartlett's present address is Dept. 865, IBM Canada, 101 Valleybrook, Toronto, Ontario, Canada.

agreeing with the various models, has a length of $\approx 0.4\ d$ (13). It has been claimed however, that the overlap region may be as much as $0.6\ d$ (14).

A precise determination of the electron density profile from x-ray diffraction data could be correlated with similar profiles calculated from the knowledge of the primary sequence for each of the model assemblies that have been proposed, with the aim of determining which model is in best agreement with the experimental data. Defects in collagen structure exist in several disease conditions (15, 16). Study of these defects will be facilitated by a better knowledge of the normal structure.

Electron density profiles of the native tendon have been presented and discussed (17–22). Tomlin and Worthington (17) and Ellis and McGavin (19) assumed there was centrosymmetry. Their determination showed the expected step functions and were most useful first steps. They cannot, however, be correct in detail, because none of the proposed models would permit a centrosymmetric unit cell. Chandross and Bear (20) made the logical assumption that regions of collagen fibril that take up a positive heavy-metal stain, as revealed in the electron microscope, are intrinsically electron dense. They then related the x-ray meridional intensities of unstained collagen fibrils to the proposed electron-dense bands and produced a model and phases that resulted in the expected step function in the electron density of the unit cell. Subsequently, Hulmes et al. (21) and Claffey (22) calculated theoretical phases based on the generally accepted quarter-stagger model and the known primary sequence of the α_1-chains. Hulmes et al. (21) assumed the α_2-sequence would be homologous with that of the α_1- in the regions where the α_2-sequence had not been determined, because this has been shown to be so in those regions that have been determined. The phases calculated in these proposals did not fully agree, but both gave step functions in electron density when combined with experimentally measured x-ray intensities. The model of Hulmes et al. (21) might be expected to give somewhat better results, because it contained features (e.g., covalently bound disaccharides) not included in the simpler model used by Claffey. It has also been suggested elsewhere (23) that the phases proposed by Hulmes et al. are more accurate.

The present investigation has not assumed that the unit cell is centrosymmetric. Low angle x-ray diffraction patterns from normal wet tendons and wet tendons isomorphously stained with heavy metals, together with electron micrographs of the same material, have been used to attempt to determine the intensities and phases of all reflections up to the 10th order from the basic unit cell. To localize the heavy metal by electron microscopy, the material had to be fixed. Complications introduced by the fixative prevented phasing of some orders. Where solutions were obtained, there was good agreement with the phases proposed by Hulmes et al. (21). Our experimental evidence thus supports their theoretically derived phases.

MATERIALS AND METHODS

Gastrocnemius tendons were removed for 18-d-old healthy male Pekin ducks after cervical dislocation. Meridional x-ray diffraction patterns were obtained from native wet tendons and again after the tendons were stained by a variety of methods described later. The stained tendons were also used in the wet state.

Diffraction patterns were collected at two facilities, with excellent agreement. At Guelph, Cu $K\alpha_1$ radiation was obtained from a sealed tube source with the aid of a focusing quartz-crystal monochromator and an appropriate slit system. Detection of well-resolved orders was obtained at a sample-to-detector distance of 1 m with a Tennelec linear position-sensitive detector (Tennelec, Inc., Oak Ridge,

Tenn.). At Oak Ridge a 10-m small-angle scattering camera (24) was used. The apparatus utilizes a 6-kW rotating anode x-ray generator (Cu Kα radiation), a compression-annealed pyrolytic graphite monochromator, pin-hole collimation, and a two-dimensional, position-sensitive detector. Typical diffraction patterns from both instruments are shown in Fig. 1. After background correction, the intensities were corrected for geometric effects by the method of Wang and Worthington (25). With reasonable values for our sample parameters and with division by a normalization factor, the following multiplicative factor can be obtained from the equation of Wang and Worthington.

$$C(h) = \left[\frac{R^2 + \frac{h^2\omega^2}{d^2}}{R^2}\right]^{1/2},$$

where R is the radius of the disk in reciprocal space, d is the axial period, h is the order of diffraction, and ω the mean angle of disorientation. The latter can be determined directly from the data obtained with a two-dimensional, position-sensitive detector, as shown in Fig. 1. $R \simeq 10^{-3}$ Å^{-1} and $\omega \simeq 10^{-1}$ radian for our samples. With these values the correction factor increased from 1.01 for $h = 1$ to 1.78 for $h = 10$. Lorentz and polarization corrections were not applied because they were considered negligible (26).

After diffraction patterns were obtained from the native wet tendons, some tendons were subsequently stained with either phosphotungstic acid (PTA) or uranyl acetate (UA), following the techniques and concentrations outlined by Ellis and McGavin (19). Samples were thoroughly washed in distilled water for 6 h after staining to preclude any negative staining. The binding of PTA in positive staining indicates the positions of polar groups such as arginine residues, whereas UA stains anionic groups. Moreover, both stains are particularly suitable for obtaining electron micrographs of the collagen fibrils. In addition, some tendons were fixed with glutaraldehyde and still others with both glutaraldehyde and osmic acid before heavy-metal staining.

After diffraction experiments with the stained tendons, the samples were prepared, sectioned, and examined with the electron microsocpe to determine the location and intensity of the heavy metals.

Those samples that were fixed before staining were treated as follows: (*a*) 2 h in 3% glutaraldehyde in Sörensen's isotonic buffer at pH 7.2–7.3; (*b*) at least 2 hr (usually overnight) in isotonic phosphate buffer (pH 7.2–7.3) with at least 1 change; (*c*) 2 h in 1% osmic acid in Millonig's phosphate buffer (pH 7.2–7.3) with sucrose; (*d*) at least 1 hr in Millonig's buffer with at least 1 change (steps [*c*] and [*d*] were omitted for some samples); (*e*) soaked for 24 h in either (*i*) 1% UA in 30% ethanol in water, or (*ii*) 1–2% PTA in 30% ethanol in water; and (*f*) washed for 24 h with ethanol water mix. Diffraction patterns were obtained at this point. Then (*g*) dehydration was accomplished by removing half of the 30% ethanol in water mix and adding an equivalent amount of 90% alcohol. This was repeated until no "convection currents" could be seen when a drop of 90% ethanol was added (usually 8 or 9 times at 15 min each with occasional mixing). (*h*) 100% ethanol for 15 min (twice); (*i*) half propylene oxide, half 100% ethanol for 10–15 min (twice); (*j*) propylene oxide for 10 min (twice); (*k*) half propylene oxide, half Epon (Shell Chemical Co., Houston, Tex.) for at least 1 h. (*l*) pure Epon cured according to Luft (27) as follows: (*i*) 35°C for 12 h; (*ii*) 45°C for 12–16 hr; and (*iii*) 65°C for 12 h, or until block is sufficiently hard. Steps (*e*) and (*f*) were omitted for those samples stained before fixation. Step (*k*) was performed at room temperature, whereas steps with alcohol (*h, i,* and *j*) were performed in an ice bath.

A typical region of PTA-stained tendon (fixed with glutaralehyde) is shown as a transmission electron micrograph in Fig. 2. An average densitometer trace of a transmission electron micrograph of a sample fixed with glutaraldehyde and stained with PTA is shown in Fig. 3. Note that bands a_2, c_2, and b_1 were not observed, whereas a_4 and c_3 showed up only as shoulders on neighboring bands. The trace is an average over 20 unit cells from different areas of the tissue. The deviations of individual cells from the mean was small. The film used was Eastman Kodak, type 5302, (Eastman Kodak Co., Rochester, N.Y.).

The Patterson map (to be described later) may be generated from the electron micrograph on the assumption that the differences in optical density vary with the number of staining atoms at given locations within the unit cell of the sample. The optical density of the particular film used as a function

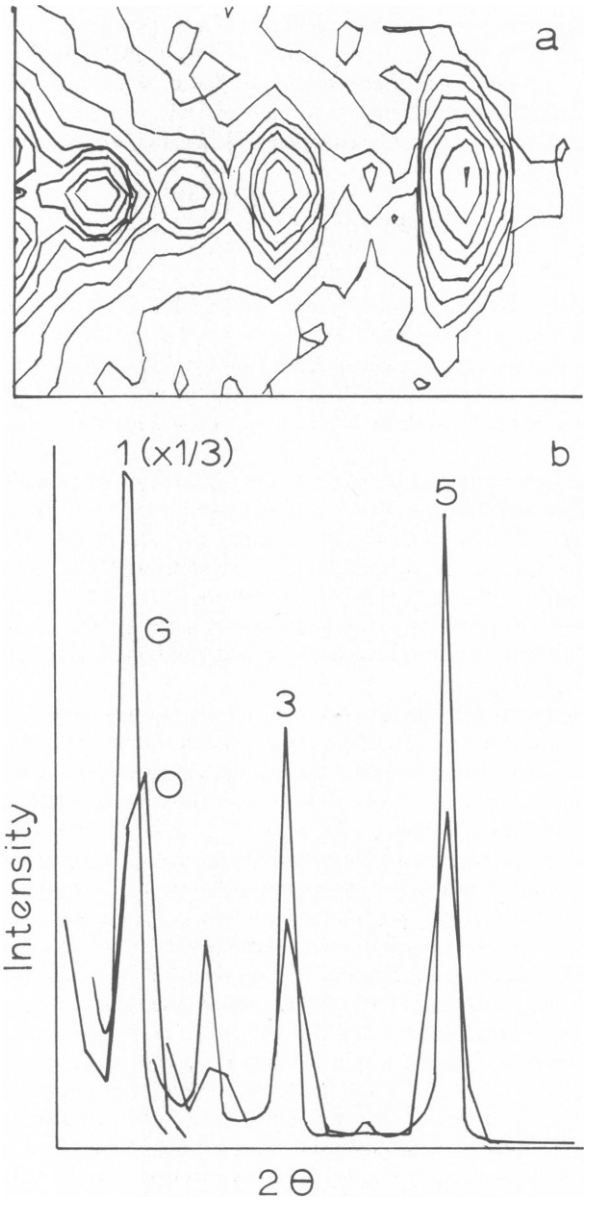

FIGURE 1 Comparison of diffraction patterns obtained at Oak Ridge with the two-dimensional detector and at Guelph with a one-dimensional detector. Both sets of data were obtained with the same sample, i.e., wet collagen stained with PTA. For convenience, only the right sides of the symmetrical patterns are shown. (*a*) Initial two-dimensional plot with Oak Ridge system. (*b*) Integration of Oak Ridge data (the broader, lower peaks, labeled 0) compared with Guelph data, labeled G. Data sets are normalized to the same total area each. No other corrections are applied. The relative intensities of the first six orders for the Guelph data are: 321; 24; 68; 2; 100; and 0. For the Oak Ridge data, the corresponding figures are: 345; 17; 54; 1; 98; and 0.

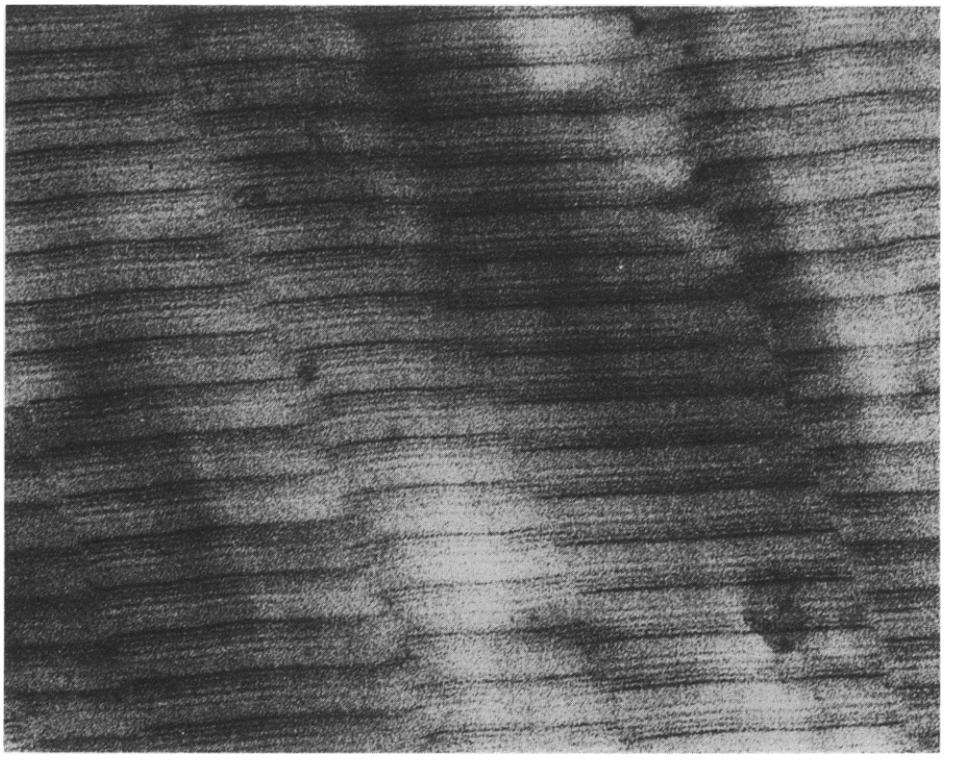

FIGURE 2 Transmission electron micrograph (× 166,850) of collagen, glutaraldehyde-fixed, PTA-stained.

of incident electron intensity is not known to us. Within the range of optical densities encountered, film response is approximately linear with respect to the logarithm of the exposure (28). Consequently, it can be shown that the optical density will be an approximately linear funtion of the number of heavy atoms at a given location within the sample.

The corrected structure factors from diffraction data for tendons treated by a variety of methods are

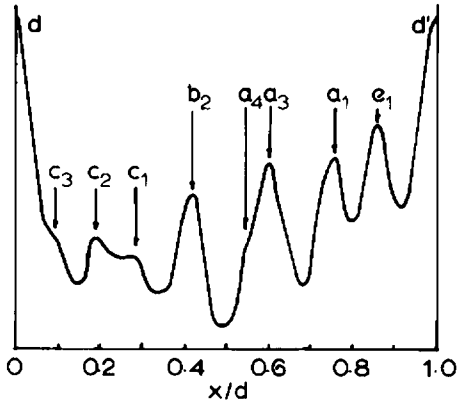

FIGURE 3 Densitometer trace of electron micrograph of collagen fixed with glutaraldehyde and stained with PTA. The trace is an average over 20 unit cells.

TABLE I
STRUCTURE FACTOR MAGNITUDES FOR X-RAY DIFFRACTION FROM WET DUCK TENDONS WITH VARIOUS TREATMENTS

Order numbers	Untreated	+G	+G+O	+PTA	+G+PTA	+G+O +PTA	+UA	+G+UA	+G+O +UA
1	535	373	167	158	158	213	129	93	149
2	29	48	16	44	44	32	56	51	48
3	168	84	72	76	72	50	32	16	13
4	19	46	29	14	24	19	26	19	14
5	100	100	100	100	100	100	100	100	100
6	31	100	40	0	6	71	49	76	82
7	57	64	52	70	56	62	95	91	75
8	27	29	19	45	35	50	42	23	16
9	68	97	53	49	70	88	65	93	93
10	27	55	34	24	54	60	29	51	54

G is glutaraldehyde fixed, O is osmic acid fixed, PTA is phosphotungstic acid, and UA is uranyl acetate.

presented in Table I. Each set, for the first six orders, is an average of three experiments at Guelph and one at Oak Ridge. For orders 7–10, three experiments at Guelph were averaged. Measurements beyond the sixth order were not made at Oak Ridge. The data are normalized by setting fifth-order structure factors equal to 100. It can be seen that the very presence of the fixative alters the diffraction pattern. The alteration was more profound when osmium fixation was use in addition to glutaraldehyde.

Fixation with glutaraldehyde alone or with osmic acid before staining with UA changed the structure factors for almost all orders. In addition, the electron micrographs of UA-stained material showed significantly less detail than those for PTA. In spite of prolonged washing after staining, areas with considerable negative staining were always present. The banding patterns were much less distinct and we were unable to identify bands with any confidence. Consequently, the UA data could not be used for phasing purposes.

The integrated intensities of the diffraction peaks had errors in them not only due to counting statistics, but also due to systematic errors associated with errors in the multiplicative correction factor, background subtraction, etc. These were all considered in the calculation of the uncertainties in the final phase assignments.

DATA ANALYSIS

The electron density may be expressed as:

$$\rho(x) = \frac{2}{L}\sum_h |F_h| \cos(2\pi hx - \alpha_h),$$

where L is the length of the unit cell, x is the fractional position along the cell, α_h is the phase angle, and F_h is the structure factor for the h^{th} order. The relative magnitudes of $|F_h|$ are proportional to the square root of the corrected intensities from the diffraction pattern.

The phase angles cannot be obtained directly from the diffraction pattern. However, if diffraction patterns from the isomorphous replacement of two heavy metals are obtained, the phases can be calculated if one knows the locations, and consequently the phases, of the heavy metals. In principle, inspection of the Patterson maps generated by

$$P(U) = \frac{2}{L}\sum_h |F(h)|^2 \cos 2\pi hU,$$

where L is the length of the Patterson unit cell and U is the fractional position of the metal-metal vectors, will reveal the positions of the heavy-metal stains. Patterson maps from the x-ray diffraction data of samples stained with UA and PTA were sufficiently featureless, due to overlapping of Patterson peaks, that the locations of the heavy-metal stains could not be adequately determined.

As a refinement, difference Patterson maps, defined by

$$P(U) = \frac{2}{L} \sum_h \{ |F(h)_{\text{stain}}|^2 - |F(h)_{\text{stain}}^{\text{no}}|^2 \} \cos(2\pi hU),$$

were used to better reveal heavy-metal positions, but even these were inadequate. Examination of electron micrographs showed multiplicity of stain locations in the unit cell.

To overcome these difficulties, densitometer tracings of positively stained electron micrographs of collagen were used to find the relative positions and amounts of heavy-metal stain along the unit cell. Because only the stain is revealed on the electron micrograph, the densitometer tracing from this was used as the electron density of stain alone, and substituted into the pair correlation expression for the Patterson map:

$$P(u) = L \int_0^L \rho(x)\rho(x + u)\, dx.$$

This was then compared with the difference Patterson map as previously obtained from diffraction data of stained and unstained collagen. One would expect the difference Patterson map from diffraction data to be similar to the Patterson map from the electron micrograph, because both depend upon the distribution of heavy atoms within the unit cell. If reasonable correspondence is obtained, this increases confidence in the use of phases determined by this method.

The difference Patterson from diffraction data cannot be identical to the Patterson map from electron microscopy because, as has been pointed out by Ramachandran and Srinivasan (29), the diffraction difference Patterson map will contain cross-terms due to interactions between the native material and the staining atoms. They have also emphasized (p. 139) that if the isomorphism is of the additive type, the only advantage to be gained from a difference Patterson is an appreciable reduction of background.

The diffraction pattern that might be expected from the stain alone was calculated by using the densitometer tracing in the following structure-factor equation:

$$F_H(h) = \int_0^L \rho_H(x) \exp\{2\pi ihx\}\, dx = |F_H(h)|\, e^{i\alpha_H(h)},$$

where H denotes quantities referring to stain alone for each order of the diffraction pattern of stained collagen. The individual contributions to the structure factor from the collagen and stain alone were separated as follows:

$$|F_s(h)|\, e^{i\alpha_s(h)} = |F_c(h)|\, e^{i\alpha_c(h)} + |F_H(h)|\, e^{i\alpha_H(h)},$$

where s denotes quantities referring to stained collagen and c to collagen alone. In the ideal case for each order, these three quantities would be drawn on an Argand diagram and, by using standard construction (30), two solutions for $\alpha_c(h)$ would be sought from the data of each stain. A single-phase solution is required for each order, and the solution is taken as the

common phase between the two pairs of solutions. The phase for each order thus determined enables calculation of the electron density distribution along the unit cell of unstained collagen.

The H data is obtained from the densitometer tracing of the electron micrograph, whereas the c and s data are from diffraction patterns. These must be correctly scaled relative to one another for the above construction to be meaningful; therefore, the H data were kept constant, whereas the c and s data were scaled relative to it. The c and s data were also scaled relative to one another, as the absorption of x rays in the stained samples was uncertain. Ideally, the diffraction data scaling factors for collagen and stained collagen were those values that a computerized search revealed as best satisfying the following two criteria. For any value of the scaling factors, the first condition that must be met is that the vectorial addition, $\mathbf{F}_s = \mathbf{F}_c + \mathbf{F}_H$, must be possible for as many orders as possible. This restricted the values of the scaling factors to within certain limits. The second condition that must ideally be met is that out of the pairs of solutions for α_C for each stain, a common solution must be available for as many orders as possible. As mentioned earlier, difficulties with the UA electron micrographs precluded the use of this data. Consequently we used the PTA data only to obtain two solutions for nine of the 10 orders, and then selected the solution from each pair that was consistent with the theoretical predictions of Hulmes et al.(21)

The absolute intensities of the diffraction patterns could not be precisely determined, but for the fifth orders, the structure factor for PTA-stained collagen was approximately four times that from native collagen. The scaling factors that provided a fit were in approximately this ratio. The absolute values of the structure factors in glutaraldehyde-fixed collagen were significantly less than in the native collagen. In calculating the phase solutions, by using locally written computer programs, the errors previously mentioned were taken into account when the construction was performed. The final phase solutions, therefore, also had associated errors.

RESULTS

Samples fixed for electron microscopy after staining provided micrographs of poor quality. Moreover, the stain location and intensities of the heavy metals (as revealed in densitometer tracings) yielded Patterson functions that were very different from the Patterson functions obtained from those generated from the x-ray diffraction data. This suggested that the stain locations, as seen in the tissue fixed for the electron micrograph after staining, were not those seen by the x-rays before fixation. This cast severe doubt on the usefulness of a procedure that was very promising in principle. Nevertheless, we proceeded with the data interpretation as initially outlined. The sixth order could not be phased, a few orders had ambiguous solutions, and none of the possible phase combinations led to an electron density distribution with a well-defined step function, as would be expected due to the presence of hole and overlap regions.

The procedure was then repeated with tendons that had been fixed before staining. In this procedure, the agreement in the Patterson maps (Fig. 4) suggested that the PTA locations from electron micrographs were the same as in native stained tendon. Thus, as explained in subsequent paragraphs, we were able to phase the collagen reflections using F_H values from

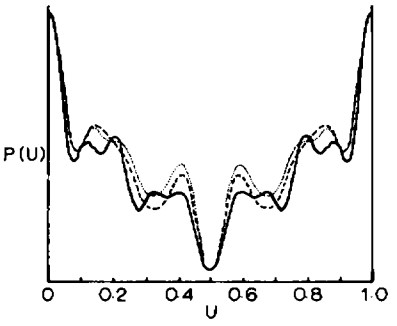

FIGURE 4 Patterson functions for wet PTA-stained collagen. The broken line is calculated to the 10th order resolution from the densitometer trace of Fig. 3 (i.e., tendon fixed with glutaraldehyde and then stained with PTA). The solid line is a difference Patterson for PTA obtained from the differences in the x-ray diffraction patterns for tendon fixed with glutaraldehyde with and without PTA. The dotted line is a difference Patterson for PTA based on x-ray diffraction patterns for unfixed tendon with and without PTA. As noted in the text, these are expected to be similar, but not identical. Poorest agreement is obtained with the fixed tendon (solid line). This may reflect the presence of additional cross-terms due to the presence of glutaraldehyde.

micrographs, F_c values from diffraction from wet native tendons, and F_s values from wet, stained, unfixed tendons.

The pattern of bands in the electron micrographs of glutaraldehyde-fixed, PTA-stained collagen is not as well-resolved as some of the excellent micrographs published elsewhere (9,31,32), which are however, obtained with collagen stained with both PTA and UA. Also, these better patterns are obtained with thin sections that had been stained (9), or with individual fibrils (31), or with reconstituted fibrils (32). In this report it was imperative that the electron micrographs be from the same material from which the diffraction pattern had been obtained. PTA staining alone could not be expected to yield the same pattern, as seen with both PTA and UA, because the distributions of anionic and cationic groups along the unit cell, although similar, are not identical. Moreover, the double staining gives further intensification by allowing uranyl anions to bind to PTA cations present in the charged regions (33). Micrographs of collagen stained with PTA only can be found (34); however, these are obtained with reconstituted fibrils and so do not represent collagen in the native state.

The locations of the bands as a percentage of the distance along the unit cell are compared with similar locations published elsewhere (9) and tabulated in Table II. To confirm our assignment of the d-band and the directions along the unit cell, all other possibilities were checked in the phasing routine, with no agreement with the phases of Hulmes et al. (21) being obtained in any case. The structure factors for the heavy metal and their relative phases are obtained independently of the band assignment, which is required only to permit us to begin our phasing at the center of the overlap region for comparison with Hulmes et al. (21), who had used the same starting point. Fig. 2 and Table II both start at the d-band, which is located in the hole region.

There have been suggestions that sample shrinkage during preparation for electron microscopy is nonlinear, resulting in a shifting of the relative locations of the stain in the

TABLE II
LOCATION OF BANDS IN ELECTRON MICROGRAPHS OF POSITIVELY STAINED COLLAGEN. LOCATION EXPRESSED AS A PERCENTAGE OF THE DISTANCE ALONG THE UNIT CELL

Band	PTA+UA*	PTA only‡
d	0	0
c_3	9	9
c_2	17	18
c_1	28	28
b_2	38	40
b_1	47	
a_4	56	54
a_3	61	60
a_2	68	
a_1	74	76
e_2	80	
e_1	87	86
d′	100	100

*From Bruns and Gross (9).
‡This report.

electron microscope sample with respect to the same in a wet, stained tendon. We have, however, compared the relative intensities of diffraction order from a dry (shrunken) tendon with those from a tendon that was held in a stretching device while drying. Under these conditions, the *d*-spacing of the unshrunken dry tendon was identical with that of a wet tendon, and the relative intensities of both dry tendons were identical. The *d*-spacing (640 Å) of the dry shrunken tendon is approximately the same as that seen in the electron micrograph. The tendons used for diffraction were dried at room temperature and thus not subjected to the extreme vacuum of the electron microscope stage, where the samples would also normally be fixed and embedded. Although this experiment is not conclusive, we interpret it as suggesting that the shrinkage occurring in the electron microscope samples is uniform and that the relative locations determined from them can be used for phase determinations.

As noted earlier, the Patterson function for PTA, as generated from the electron micrograph, should (at the same resolution) be similar to, but not identical with, the difference Patterson calculated from the x-ray diffraction patterns from the tendons with and without glutaraldehyde fixation and with and without PTA. This is demonstrated in Fig. 4, where it can be seen that the agreement is reasonable for the unfixed tendon. The agreement is poorer with the fixed tendon, perhaps because of additional cross-terms introduced by the presence of the fixative itself. The agreement between the x-ray data for unfixed tendon and that from the electron microscope supports our assumption that the distribution of PTA in unfixed wet collagen fibrils is identical to the distribution of PTA in fibrils that have been fixed, stained, dehydrated, and embedded in Epon.

The structure factors and phases for the PTA are presented together with the theoretical phases for the collagen reflections as calculated by Hulmes et al. (21) in Table III. Experimental phases are also listed for the nine orders where a fit was obtained. For consistency, all phases are calculated from the center of the overlap band, as in the initial calculations (21).

TABLE III

HEAVY METAL DATA AND A COMPARISON OF EXPERIMENTAL AND THEORETICAL PHASES FOR COLLAGEN X-RAY REFLECTIONS

Order	From electron micrograph		Experimental	Theoretical*
	F_H	α_H	α_c	α_c
1	140	243	7 ± 15°	12°
2	57	88	314 ± 57°	335°
3	57	280	182 ± 18°	179°
4	22	94	250 ± 37°	246°
5	100	316	55 ± 58°	4°
6	29	19		278°
7	72	2	105 ± 70°	157°
8	38	243	288 ± 56°	253°
9	44	149	240 ± 41°	278°
10	13	306	354 ± 20°	348°

*From Hulmes et al. (21).

Relative electron density distributions of native wet collagen are shown in Fig. 5. Both are calculated by using our intensities. In one case, the phases suggested by Hulmes et al. (21) are used for all orders, and in the other, a combination of the Hulmes et al. phase for the sixth order and of our phases for the other nine orders is used. Our intensities from avian tendon are very similar to those from mammalian tendon. The avian intensities show a slightly greater contrast between the stronger odd orders and the weaker even orders than do mammalian intensities.

DISCUSSION

Complete phasing by using electron micrographs to locate isomorphously added heavy atoms was not achieved when fixation of tendons followed heavy-metal staining, because we were

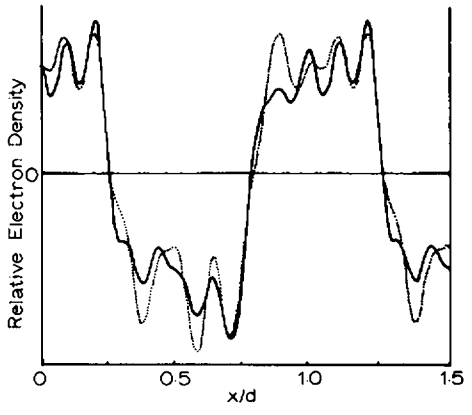

FIGURE 5. Relative electron density distribution for wet native collagen in avian tendon. One and a half unit cells are shown. The solid line is based entirely on phases proposed by Hulmes et al. (21), and the dotted line is based on phases developed in this report, i.e., all phases except for the sixth order. The phase proposed by Hulmes et al. for the sixth order has been used. It should be noted that this figure starts at the center of the overlap region (the point relative to which phases were developed), whereas Fig. 3 started at the d-band, which is in the hole region.

unable to obtain good quality electron micrographs with tendons fixed after staining. Moreover, it appeared that in the post-staining fixation process the original PTA distribution was altered.

When tendons were fixed with glutaraldehyde or glutaraldehyde and osmic acid before staining, we could obtain much better electron micrographs without any evidence of PTA redistribution. Electron micrographs of UA-stained material showed considerable negative staining in places and lacked sufficient sharpness to adequately define the stain locations. Consequently, the use of only one stain led to ambiguous solutions for 9 of the 1st 10 orders. The 6th order could not be phased. For each of the nine phased orders one of the two possible solutions agreed with the phases proposed by Hulmes et al. (21), which were obtained by calculations based on a reasonable model of the unit cell of the collagen fibril.

As the experimentally derived phases generally agree with the theoretical phases, we suggest that all phases proposed by Hulmes et al. are probably correct.

The electron density distributions calculated by using our intensities and either the phases of Hulmes et al. or a combination of our phases and theirs both show an overlap region of 48% of the length of the unit cell. This is, depending on the conformation of the telopeptides, well within the range that could be expected, and is in good agreement with the 47% prediction of Hulmes et al. (21) and Tomlin and Worthington (17), and the 46% value predicted by Chandross and Bear (20).

The Patterson function generated from the x-ray diffraction data shows a V-shaped, almost ripple-free function with a short section of zero amplitude in the center. This is entirely consistent with a step function with a 48% overlap region.

It is rather surprising that three of the bands (a_2, b_1, and e_2) did not appear in the electron micrograph of the PTA-stained material, because all band locations contain groups that would be expected to bind PTA (35). However, in the native tissues, there are significant quantities of proteoglycans and glycosaminoglycans that are associated with the collagen fibrils and that have charge groups similar to the PTA. These might be bound to some sites, thus blocking them from PTA. Doyle et al. (36) have summarized the evidence from several papers that used ruthenium red or bismuth nitrate to locate glycosaminoglycans, and found a strong tendency for these to collect in the region of those bands that did not stain with PTA.

We are indebted to Diane Barker for technical assistance, and to Dr. David Inman of McMaster University for assistance with electron microscopy.

This research was sponsored by the National Research Council of Canada, The Muscular Dystrophy Association of Canada, and the Division of Materials Science, U.S. Department of Energy under contract W-7405-eng-26 with Union Carbide Corporation.

Received for publication 24 August 1978 and in revised form 4 December 1978.

REFERENCES

1. RAMACHANDRAN, G. N. 1967. Treatise on Collagen. Academic Press Inc. Ltd., London and New York. Vol 1. 556.
2. RICH, A., and F. H. C. CRICK. 1961. The molecular structure of collagen. *J. Mol. Biol.* 3:483.
3. HULMES, D. J. S., A. MILLER, D. A. D. PARRY, K. A. PIEZ, and J. WOODHEAD-GALLOWAY. 1973. Analysis of the primary structure of collagen for the origins of molecular packing. *J. Mol. Biol.* **79**:137.
4. DIXIT, S. N., J. M. SEYER, and A. H. KANG. 1977. Covalent structure of collagen: Amino-acid sequence of

chymotryptic peptides from the carboxyl-terminal region of α2-CB3 of chick-skin collagen. *Eur. J. Biochem.* **81**:599.
5. HODGE, A. J., and J. A. PETRUSKA. 1963. *In* Aspects of Protein Structure. G. N. Ramachandran, editor. Academic Press Inc., New York. 289.
6. DOYLE, B. B., D. W. L. HUKINS, D. J. S. HULMES, A. MILLER, C. J. RATTEW, and J. WOODHEAD-GALLOWAY. 1974. Origins and implications of D-stagger in collagen. *Biochem. Biophys. Res. Commun.* **60**:858.
7. SMITH, J. W. 1968. Molecular pattern in native collagen. *Nature (Lond.).* **219**:157.
8. DOYLE, B. B., D. J. S. HULMES, A. MILLER, D. A. D. PARRY, K. A. PIEZ, and J. WOODHEAD-GALLOWAY. 1974. D-periodic narrow filament in collagen. *Proc. R. Soc. Lond. B. Biol. Sci.* **186**:67.
9. BRUNS, R. R., and J. GROSS. 1974. High resolution analysis of the modified quarter-stagger model of the collagen fibril. *Biopolymers.* **13**:931.
10. GRANT, R. A., R. W. HORNE, R. W. COX. 1965. New model for the tropocollagen macromolecule and its mode of aggregation. *Nature (Lond.).* **207**:822.
11. VEIS, A., and L. YUAN. 1974. A four strand overlap model for the collagen microfibril. *Fed. Proc.* **33**:1596.
12. HOSEMANN, R., W. DREISSIG, and T. NEMETSCHEK. 1974. Schachtelhalm - structure of the octafibrils in collagen. *J. Mol. Biol.* **83**: 275.
13. COX, R. W., and R. A. GRANT. 1969. Structure of collagen fibril. *Clin. Orthop. Relat. Res.* **67**: 175.
14. SPADARO, J. A. 1970. Structural implications of banding in unstained collagen. *Nature (Lond.).* **228**: 79.
15. BARTLETT, M. W., P. A. EGELSTAFF, T. M. HOLDEN, R. H. STINSON, and P. R. SWEENY. 1973. Structural changes in tendon collagen resulting from muscular dystrophy. *Biochim Biophys. Acta.* **328**:213.
16. BORNSTEIN, P. 1974. Biosynthesis of collagen. *Annu. Rev. Biochem.* **43**:567.
17. TOMLIN, S. G., and C. R. WORTHINGTON, 1956. Low-angle X-ray diffraction patterns of collagen. *Proc. R. Soc. Lond. A. Math. Phys. Sci.* **235**:189.
18. ERICSON, L. G., and S. G. TOMLIN. 1959. Further studies of low-angle X-ray diffraction patterns of collagen. *Proc. R. Soc. Lond. A. Math. Phys. Sci.* **252**:197.
19. ELLIS, D. O., and S. MCGAVIN. 1970. The structure of collagen—an X-ray study. *J. Ultrastruct. Res.* **32**:191.
20. CHANDROSS, R. J., and R. S. BEAR. 1973. Improved profiles of electron density distribution along collagen fibrils. *Biophys. J.* **13**:1030.
21. HULMES. D. J. S., A. Miller, S. W. WHITE, and B. B. DOYLE. 1977. Interpretation of meridional X-ray diffraction pattern from collagen-fibers in terms of known amino-acid sequence. *J. Mol. Biol.* **110**:643.
22. CLAFFEY, W. 1977. Interpretation of the small-angle X-ray diffraction of collagen in view of the primary structure of the αl chain. *Biophys. J.* **19**:63.
23. LAM, R., W. J. CLAFFEY, and P. H. GEIL. 1978. Small angle X-ray diffraction studies of mucopolysaccarides in collagen. *Biophys. J.* **24**:613.
24. HENDRICKS, R. W. 1978. The ORNL 10-m small-angle X-ray scattering camera. *J. Appl. Crystallogr.* **11**:15.
25. WANG, S. K., and C. R. WORTHINGTON. 1975. Low angle X-ray data processing for collagen. *Biophys. J.* **15**:322*a* (abstr.).
26. BLAUROCK, A. E., and C. R. WORTHINGTON. 1966. Treatment of low-angle X-ray data from planar and concentric multilayered structures. *Biophys. J.* **6**:305.
27. LUFT, J. H. 1961. Improvements in epoxy resin embedding methods. *J. Biophys. Biochem. Cytol.* **9**:409.
28. DIGBY, N., K. FIRTH, and R. J. HERCOCK. 1953. The photographic effect of medium energy electrons. *J. Photogr. Sci.* **1**:194.
29. RAMACHANDRAN, G. N., and R. SRINIVASAN. 1970. Fourier Methods in Crystallography. John Wiley & Sons, Inc., New York. 259.
30. GLUSKER, J. P., and K. N. TRUEBLOOD. 1972. Crystal Structure Analysis. Oxford University Press, London. 192.
31. FIETZEK, P. P., and K. KUHN. 1975. Information contained in amino acid sequence of α1(I)-chain of collagen and its consequences upon formation of triple helix, of fibrils and cross links. *Mol. Cell. Biochem.* **8**:141.
32. CHAPMAN, J. A. 1974. Staining pattern of collagen fibrils. a. Analysis of electron micrographs. *Connect. Tiss. Res.* **2**:137.
33. von der MARK, K., P. WENDT, F. REXRODT, and K. KUHN. 1970. Direct evidence for a correlation between amino acid sequence and cross striation pattern of collagen. *FEBS. (Fed. Eur. Biochem. Soc.) Lett.* **11**:105.
34. KUHN, K., and E. ZIMMER. 1961. Eigenschaften des Tropokollagen-Molekuls und deren Bedeutung für die Fibrillenbildung. *Z. Naturforsch. Teil B. Anorg. Chem. Org. Chem. Biochem. Biophys. Biol.* **16**:648.
35. DOYLE, B. B., D. L. HULMES, A. MILLER, D. A. PARRY, and K. A. PIEZ. 1974. Axially projected collagen structures. *Proc. R. Soc. B. Biol. Sci.* **37**:46.
36. DOYLE, B. B., D. W. L. HUKINS, D. J. S. HULMES, A. MILLER, and J. WOODHEAD-GALLOWAY. 1975. Collagen polymorphism: Its origins in the amino acid sequence. *J. Mol. Biol.* **91**:79.